33RD CONGRESS
OF THE INTERNATIONAL COUNCIL
OF THE AERONAUTICAL SCIENCES
STOCKHOLM, SWEDEN, 4-9 SEPTEMBER, 2022

NUMERICAL PREDICTION OF FOCUS BOOM GENERATED BY MANEUVERS

Shuo HAN[1], Yue XU[2]

[1] Chinese Aeronautical Establishment, Beijing, China
[2] Chinese Aeronautical Establishment, Beijing, China

Abstract

The acceleration from subsonic to supersonic performed by supersonic civil aircraft generates focus boom on the ground. The intensity of focus boom is several times higher than that of the cruising sonic boom, which greatly exceeds the low boom requirements for the commercial flight of supersonic civil aircraft. A numerical prediction method for sonic boom focusing based on the Lossy Nonlinear Tricomi Equation was studied and computational aeroacoustics techniques were applied to reduce the dispersion and dissipation caused by numerical method. The corresponding focus boom prediction code was developed. The developed code was verified using flight data, which proves that its ability of focus boom prediction. The influence of the atmospheric loss mechanism and the accelerating rate of flight on focus boom were investigated. The atmospheric loss mechanism can dissipate the acoustic energy in high frequency component and reduce the perceived loudness, which indicates that the atmospheric loss mechanism should be taken into consideration for sonic boom focusing prediction. For a given flight state, changing the flight path angle can lessen the intensity of focus boom on the ground, which might be a realistic method to reduce the impact of focus boom through the acceleration process.

Keywords: supersonic civil aircraft, maneuvering flight, focus boom, numerical prediction

1. General Introduction

Maneuvering (acceleration, climbing/diving, and turning, etc.) in supersonic fight can form a caustic and generate focus boom. Such caustic usually propagations to the ground, and the intensity of focus boom near caustic is greatly stronger than sonic boom produced by supersonic cruising. If the flight speed is greater than the cut-off Mach number, the acceleration maneuver will inevitably generate a focus boom on the ground. For supersonic civil aircraft with low boom configuration, sonic boom focusing will cause the perceived loudness of the ground sonic boom [1] to increase by more than 10dB [2], which will greatly weaken its low boom feature and the intensity of the ground focus sonic boom is unacceptable. Therefore, it is necessary to carry out sonic boom focusing research for supersonic maneuvering flight, which is of great significance for verifying focus boom suppression methods and low focus boom flight path planning of supersonic civil aircraft.

The research on the theory, prediction and experiment of sonic boom focusing have been carried out. Brekhovskikh [3] and Berry [4] developed caustic ray theory and catastrophe theory respectively, revealed the physical mechanism of focus waves and established corresponding mathematical model. Guiraud [5] developed the scaling law applied to the focusing amplitude factor of a step shock. Plotkin and Cantril [6] applied Guiraud's method to PCBoom. Auger and Coulouvrat [7] developed a pseudo-spectral method for solving nonlinear Tricomi equation, introduced a pseudo-time term in the equation and solved it by operator splitting method. Marchiano [8] rewrote the nonlinear Tricomi equation in acoustic potential flow, and used the shock matching method of Hayes [9] to solve it. Sescu and Afjeh [10] used the WENO scheme to solve the nonlinear Tricomi equation in conservative form, and used the Galerkin method to solve the numerical oscillation problem. Salamone [11] introduced the atmospheric loss terms into the nonlinear Tricomi equation, and obtained prediction results closer to the measured data. McDonald and Ambrosiano [12] used the shock capture scheme to solve the nonlinear Tricomi equation. NASA launched SCAMP (Superboom Caustic Analysis and Measurement Program) [2], which aims to develop a mathematical model of sonic boom focusing through flight tests, verify the corresponding numerical solution, and apply the developed method to the focus boom prediction of low boom configuration. This project studied the sonic boom focusing phenomenon through flight test and numerical analysis, and obtained relatively complete and reliable flight and acoustic data, which can be used for the verification of focus boom numerical prediction.

2. Sonic Boom Focusing Theory

For a supersonic maneuvering flight, the acoustic rays generated by the aircraft at different times may converge. The cross-sectional area of the ray tube is zero, and a caustic occurs. Figure 1 is a sketch of the sonic boom focusing during supersonic acceleration. The aircraft accelerates from left to right, and the acceleration reduces the Mach angle. The rays emitted at different times gradually converge to form the caustic. Above the caustics is the focus zone. There are two waves passing through each position on the caustic, which are the incoming wave and the outgoing wave. Below the caustic is the shadow zone, and the rays will not enter this area, but according to the focusing boom theory, a small amount of sound will still penetrate the caustic and enter the sound shadow area. Since the cross-sectional area of the sound ray tube on the caustic line is zero, the sound pressure predicted by the Blokhintzev invariant is infinite, so the geometric acoustic theory is not sufficient to predict the focus boom near the caustic dominated by diffraction effects.

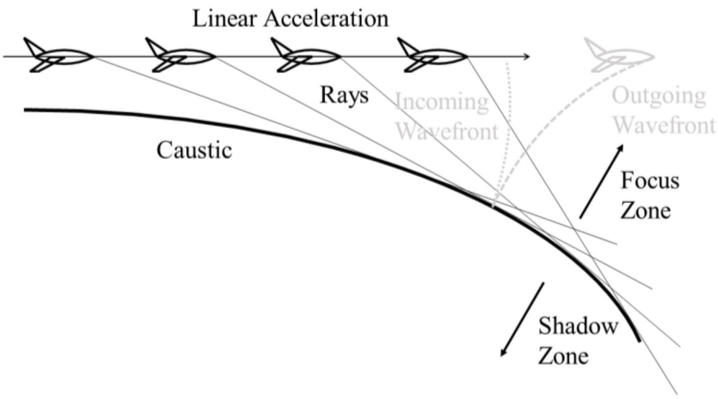

Figure 1 – Sonic boom focusing for supersonic acceleration maneuvering flight.

Figure 2 shows the rays and local coordinate near a caustic. When the sound ray propagates to the caustic, the cross-sectional area of the sound ray tube is zero, and the coordinate of this point is O. The axis perpendicular to the caustic through point O is the z-axis, the axis tangent to the caustic through point O is the x-axis, and the y-axis is right-handed with the x-axis and the z-axis. The radius of curvature of the ray passing at point O is R_{ray}, and the radius of curvature of caustics at point O is R_{cau}. Focus boom numerical prediction is based on this local coordinate.

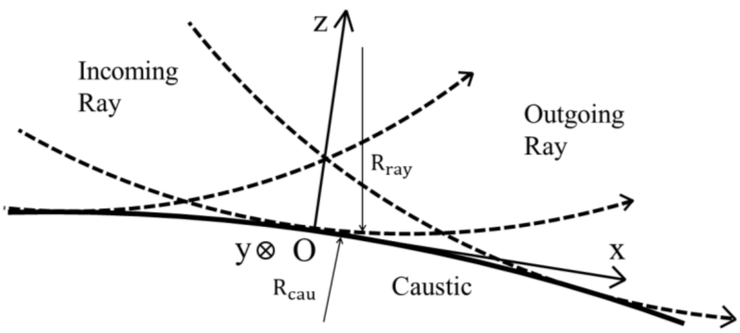

Figure 2 – Rays and local coordinate near a caustic

The phenomenon of sonic boom focusing can be described by Lossy Nonlinear Tricomi Equation (LNTE) with atmospheric loss characteristics, and its dimensionless form is:

$$\frac{\partial^2\bar{p}}{\partial\bar{z}^2}-\bar{z}\frac{\partial^2\bar{p}}{\partial\bar{t}^2}-2\frac{M_z}{\varepsilon}\frac{\partial^2\bar{p}}{\partial\bar{t}\partial\bar{z}}+\left(\frac{2M_x}{\varepsilon^2}-\frac{M_x^2}{\varepsilon^2}\right)\frac{\partial^2\bar{p}}{\partial\bar{t}^2}+\frac{\beta M_{ac}}{\varepsilon^2}\frac{\partial^2\bar{p}^2}{\partial\bar{t}^2}+\left(\frac{\bar{\alpha}}{\varepsilon^2}+\sum_{\nu=1,2}\frac{\frac{\bar{\theta}_\nu}{\varepsilon^2}}{1+\bar{\tau}\frac{\partial}{\partial\bar{t}}}\right)\frac{\partial^3\bar{p}}{\partial\bar{t}^3}=0 \tag{1}$$

The first and second terms on the left side of the equation are diffraction effect, the third term is atmospheric wind effect in z direction, the fourth term is atmospheric wind effect in x direction, the fifth term is nonlinear effect, and the sixth term is atmospheric thermal viscous absorption and molecular relaxation effects. LNTE ignores acoustic diffraction effects in the y-direction and assumes that within the focal zone, the sonic boom propagates mainly in x-z plane.

In LNTE, $\bar{p}=p/p_{ac}$ is dimensionless sound pressure, p_{ac} is characteristic sound pressure. The dimensionless normal distance to the caustics:

$$\bar{z}=\frac{z}{d}=\left(\frac{2f_{ac}^2}{R_{tot}c_0^2}\right)^{\frac{1}{3}} \tag{2}$$

is the ratio of the normal distance to the caustics to the thickness of the acoustic diffraction boundary layer, in which $f_{ac}=1/t_{ac}$, t_{ac} is characteristic time, and c_0 is ambient sound speed. The relationship between R_{tot}, radius of caustic curvature R_{cau} and radius of ray curvature R_{ray}:

$$\frac{1}{R_{tot}}=\frac{1}{R_{cau}}-\frac{1}{R_{ray}} \tag{3}$$

$\bar{t}$ is dimensionless time:

$$\bar{t}=f_{ac}\left[t-\frac{x\left(1-\frac{z}{R_{ray}}\right)}{c_0}\right] \tag{4}$$

$M_z=v_z/c_0$ is the dimensionless atmospheric wind speed in the z direction. The diffraction coefficient:

$$\varepsilon=\frac{\lambda_{ac}}{d}=\lambda_{ac}\left(\frac{R_{tot}c_0^2}{2f_{ac}^2}\right)^{-\frac{1}{3}}=\left(\frac{\lambda_{ac}}{R_{tot}}\right)^{\frac{1}{3}} \tag{5}$$

is the ratio of the wavelength of the characteristic acoustic wave to the thickness of the diffraction boundary layer. $M_x=v_x/c_0$ is the dimensionless atmospheric wind speed in the x direction. β is nonlinear coefficient. $\bar{\alpha}=\delta f_{ac}/c_0^2$ is dimensionless thermal viscous absorption coefficient. $\upsilon=1,2$ in the summation sign of the last term represents the molecular relaxation effect of oxygen and nitrogen respectively. $\bar{\theta}_\upsilon=\bar{\tau}_\upsilon m_\upsilon=f_{ac}\tau_\upsilon\left(c_{\infty,0}^2-c_0^2\right)/c_0^2$ is sound dispersion coefficient. $\bar{\tau}_\upsilon=f_{ac}\tau_\upsilon$ is dimensionless molecular relaxation time.

Solving the LNTE requires setting correct boundary conditions on the time axis $\bar{t}$ and the caustic normal axis $\bar{z}$. The boundary conditions for the time axis $\bar{t}$ are that the focus boom signal is zero at negative and positive infinity:

$$\bar{p}(t\to\pm\infty,\bar{z})=0 \tag{6}$$

Along the negative semi-axis of the caustic normal axis $\bar{z}$, the sound pressure decays exponentially and goes to zero:

$$\bar{p}(\bar{t},\bar{z}\to-\infty)=0 \tag{7}$$

Along the positive semi-axis of the caustic normal axis $\bar{z}$, at a position far enough from the caustic, the focus boom signal needs to match the incoming and outgoing waves of geometric acoustics:

$$\bar{p}(\bar{t},\bar{z}\to+\infty)\approx\bar{z}^{1/4}\left[F\left(\bar{t}+\frac{2}{3}\bar{z}^{3/2}\right)+G\left(\bar{t}-\frac{2}{3}\bar{z}^{3/2}\right)\right] \tag{8}$$

where F is the incoming wave and G is the outgoing wave, both of which are dimensionless by the characteristic sound pressure. Since the outgoing wave G is the quantity to be determined, Salamone [13] derived the acoustic radiation boundary condition that only includes the positive semi-axis of incoming wave F:

$$\bar{z}^{1/4}\frac{\partial\bar{p}}{\partial\bar{t}}+\bar{z}^{-1/4}\frac{\partial\bar{p}}{\partial\bar{z}}+\bar{z}^{-5/4}\frac{\bar{p}}{4}=2F'^{\left(\bar{t}+\frac{2}{3}\bar{z}^{-3/2}\right)} \tag{9}$$

3. Numerical Prediction Method for Focus Boom

The sonic boom focusing mainly occurs in the space near the caustic, and the computational domain of LNTE should include the region dominated by the sonic boom focusing effect. The sketch of the computational domain of LNTE is shown in Figure 3. The horizontal axis of the computational domain is the time axis $\bar{t}$, which represents the phase of the focus boom signal. The range of the time axis needs to satisfy that the sound pressure at the left and right boundaries of the computational domain is zero. The vertical axis is the caustic normal axis $\bar{z}$, usually $\bar{z}_{min} = -1$ and $\bar{z}_{max} = +1$ are selected. The phase difference between the incoming wave and the outgoing wave at the upper boundary of the computational domain is about one characteristic time of the incoming sonic boom signal.

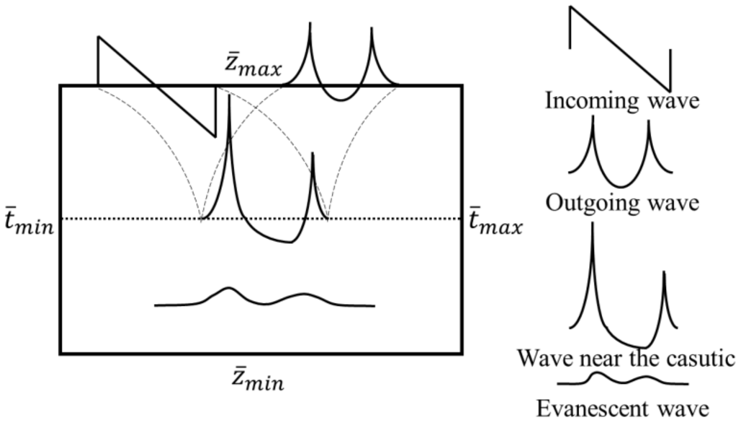

Figure 3 – Sketch of LNTE computational domain

By adding an unsteady term containing pseudo-time step $\bar{\sigma}$ to LNTE, the governing equation for numerically solving LNTE in the computational domain can be obtained:

$$\frac{\partial^2 \bar{p}}{\partial \bar{z}^2} - \bar{z}\frac{\partial^2 \bar{p}}{\partial \bar{t}^2} - 2\frac{M_z}{\varepsilon}\frac{\partial^2 \bar{p}}{\partial \bar{t}\partial \bar{z}} + \left(\frac{2M_x}{\varepsilon^2} - \frac{M_x^2}{\varepsilon^2}\right)\frac{\partial^2 \bar{p}}{\partial \bar{t}^2} + \frac{\beta M_{ac}}{\varepsilon^2}\frac{\partial^2 \bar{p}^2}{\partial \bar{t}^2} + \left(\frac{\bar{\alpha}}{\varepsilon^2} + \sum_{\nu=1,2}\frac{\frac{\bar{\theta}_\nu}{\varepsilon^2}}{1+\bar{\tau}\frac{\partial}{\partial \bar{t}}}\right)\frac{\partial^3 \bar{p}}{\partial \bar{t}^3} = \frac{\partial^2 \bar{p}}{\partial \bar{t}\partial \bar{\sigma}} \quad (10)$$

The iterative process of the governing equation is shown in Figure 4. The governing equation adopts the operator splitting method, and the diffraction effect term, nonlinear effect term, thermal viscous absorption and molecular relaxation terms are solved separately within each pseudo-time step $\bar{\sigma}_k$. Linear terms are solved in the frequency domain, and nonlinear terms are solved in the time domain. Uniform discretization is used for $\bar{t}$ and $\bar{z}$ in the computational domain. The unsteady term on the left side of the governing equation gradually tends to zero, and the solution converges.

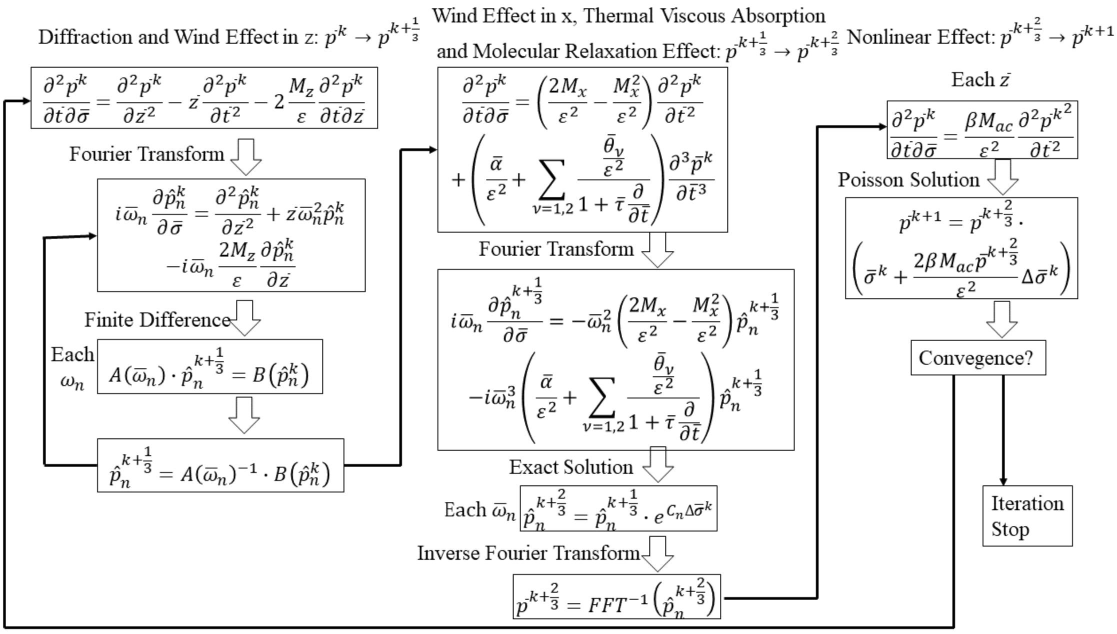

Figure 4 – LNTE algorithm

At the beginning of the iteration, the initial value of the sound pressure field in the computational domain is zero. In the k-th iteration, the first step is to solve the diffraction term and the atmospheric wind term in the z direction. Convert the sound pressure field to the frequency domain using the Fourier transform:

$$i\bar{\omega}_n \frac{\partial \hat{p}_n^k}{\partial \bar{\sigma}} = \frac{\partial \hat{p}_n^k}{\partial \bar{z}^2} + \bar{z}{\bar{\omega}_n}^2 \hat{p}_n^k - i\bar{\omega}_n \frac{2M_z}{\varepsilon}\frac{\partial \hat{p}_n^k}{\partial \bar{z}} \tag{11}$$

where i is imaginary unit, and $\bar{\omega}_n$ is the n-th dimensionless angular frequency after Fourier transform, and the corresponding harmonic sound pressure field is $\hat{p}_n^k$. There are two methods to solve this equation. The first refers to Salamone's method [13]. The equations are in the fully implicit discretization scheme, the spatial difference is in the second order scheme, and the pseudo-time difference is in the first order scheme. The second is to use CAA (Computational AeroAcoustics) to solve the equation. The spatial difference is solved using DRP (Dispersion Relation Preserving) scheme [14]. The pseudo-time difference is solved using the modified Runge-Kutta scheme [15]. These two schemes are both high order schemes with low dispersion and low dissipation feature. The equations need to be solved with the boundary conditions of the computational domain. Upper boundary condition equation is:

$$\frac{\partial \hat{p}_n^k}{\partial \bar{z}} + \left(i\bar{\omega}_n \bar{z}_{max}^{-1/2} + \frac{\bar{z}_{max}^{-1}}{4}\right)\hat{p}_n^k = \bar{z}_{max}^{-1/4}\cdot 2i\bar{\omega}_n \cdot e^{\frac{2}{3}i\bar{\omega}_n \bar{z}_{max}^{-3/2}}\cdot \hat{F}_n \tag{12}$$

$\hat{F}_n$ is Fourier transform of the incoming wave corresponds to $\bar{\omega}_n$. The spatial difference can be solved in the second order scheme or in the DRP scheme. Upper boundary condition equation:

$$\frac{\partial \hat{p}_n^k}{\partial \bar{z}} - \left(\frac{1}{4}|\bar{z}_{min}|^{-1} + |\bar{\omega}_n||\bar{z}_{min}|^{\frac{1}{2}}\right)\hat{p}_n^k = 0 \tag{13}$$

The spatial difference can be solved in the first order scheme or in the DRP scheme. The second step is to solve atmospheric wind term in the x-direction, thermal viscous absorption term and molecular relaxation term:

$$\frac{\partial \hat{p}_n^{k+\frac{1}{3}}}{\partial \bar{\sigma}} = -\bar{\omega}_n^2\left(\frac{2M_x}{\varepsilon^2} - \frac{M_x^2}{\varepsilon^2}\right)\hat{p}_n^{k+\frac{1}{3}} - \bar{\omega}_n^3\left(\frac{\bar{\alpha}}{\varepsilon^2} + \sum_{\upsilon=1,2}\frac{\frac{\bar{\theta}_\upsilon}{\varepsilon^2}}{1+\bar{\tau}\frac{\partial}{\partial \bar{t}}}\right)\hat{p}_n^{k+\frac{1}{3}} \tag{14}$$

The equation has exact solution:

$$\hat{p}_n^{k+\frac{2}{3}} = \hat{p}_n^{k+\frac{1}{3}}\cdot e^{C_n\cdot\Delta\bar{\sigma}^k} \tag{15}$$

where C_n is:

$$C_n = i\bar{\omega}_n\left(\frac{2M_x}{\varepsilon^2} - \frac{M_x^2}{\varepsilon^2}\right) - \bar{\omega}_n^2\left(\frac{\bar{\alpha}}{\varepsilon^2} + \sum_{\upsilon=1,2}\frac{\frac{\bar{\theta}_\upsilon}{\varepsilon^2}}{1+\bar{\tau}\frac{\partial}{\partial \bar{t}}}\right) \tag{16}$$

The third step is to solve the nonlinear term. Using the inverse Fourier transform, the frequency domain sound pressure field obtained in the second step is converted back into the time domain, and the nonlinear term becomes:

$$\frac{\partial^2 \bar{p}^k}{\partial \bar{t}\partial \bar{\sigma}} = \frac{\beta M_{ac}}{\varepsilon^2}\frac{\partial^2\left(\bar{p}^k\right)^2}{\partial \bar{t}^2} \tag{17}$$

The exact solution is Poisson solution:

$$\bar{p}^{k+1} = \bar{p}^{k+\frac{2}{3}}\left(\bar{\sigma}^k + \frac{2\beta M_{ac}}{\varepsilon^2}\cdot \bar{p}^{k+\frac{2}{3}}\cdot \Delta\bar{\sigma}^k\right) \tag{18}$$

The Poisson solution is solved by time shifting of the sound pressure, and the sound pressure in non-uniform time step is interpolated back to the uniform time coordinates.

After each iterative step is completed, the maximum residual error in the entire computational domain is monitored. The iteration can be considered to converge until the maximum residual error meets the threshold.

4. Numerical Validation

4.1 Validation Case Description

The focus boom prediction code CBoom_NLTE was developed. The code was verified using SCAMP flight test focus boom data [2], and the accelerating dive maneuver flight test, the "flight 1264" with "Maneuver C" is selected. Figure 5 shows the sketch of Flight condition for numerical verification.

Figure 5 – Flight condition for numerical verification [2]

The method of obtaining the incoming wave signal is shown in Figure 6. First, calculate the sound ray of incoming wave. It is the sound ray that is the one diffraction boundary layer thickness away from the intersection point of the caustic and the ground. The incoming wave signal is calculated on this ray to the upper boundary of the LNTE. Since the focus boom signals of the flight test are collected on the ground, the prediction needs to consider the ground reflection, and the ground reflection coefficient is 1.9.

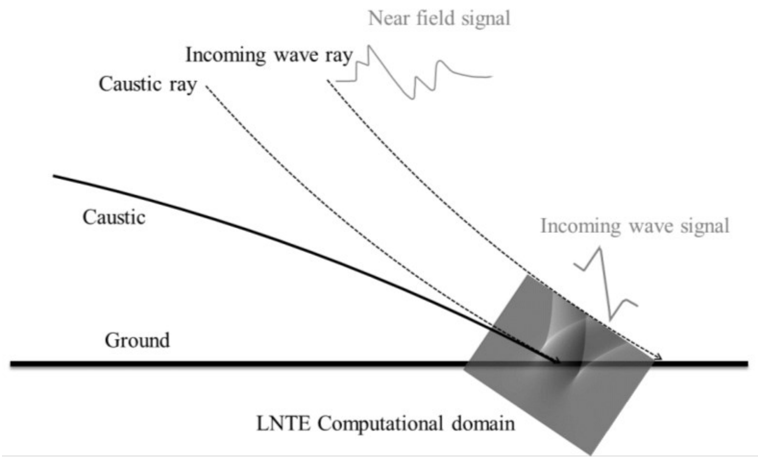

Figure 6 – Incoming wave obtaining

4.2 Prediction Results

Figure 7 is the overpressure contour in the focus boom region. The incoming wave enters the focus region from the upper left, propagates in it and penetrates the caustic slightly. The outgoing wave reflects from the caustic to the upper right and exits the focus region. The numerical prediction result shows that the maximum overpressure is at $\bar{z} > 0$, and the acoustic signal exists in $\bar{z} < 0$. These two phenomena arise from diffraction effects and contradict the geometrical acoustics, indicating that the geometric acoustic theory fails in the focus region.

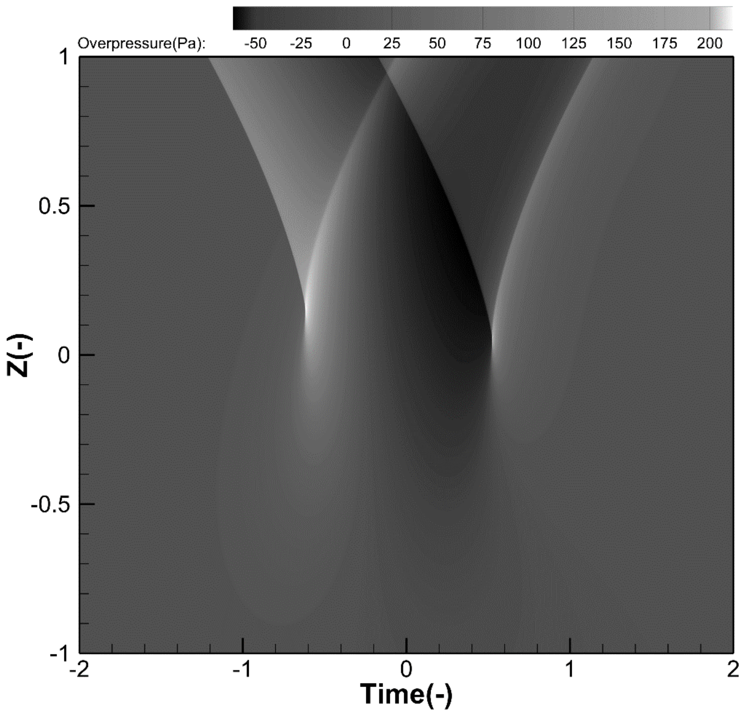

Figure 7 – Overpressure contour in the focus zone

Figure 8-11 shows the focus boom signals at four different caustic normal distances. The gray dash dot lines are the measured signals of the flight test, the blue solid lines are the predicted signals of Salamone [13], and the red solid lines are the predicted signals of CBoom_NLTE using the same method as Salamone, and the green dashed lines are the predicted signals of CBoom_NLTE using CAA. It should be notice that the atmospheric turbulence effect is not included in all the numerical predicted results.

At $\bar{z} = 0.97$, the incoming wave and outgoing wave have not yet merged, and their waveforms are maintained respectively. The numerical prediction of the incoming N-type waveform signal is in good agreement with the measured, and the maximum overpressure is slightly smaller. The two peaks of the U-shaped wave are predicted better. The prediction using the CAA are almost the same as those obtained by the low order scheme, and the three shock peaks is more accurate, and the duration of the U-shaped wave is slightly longer.

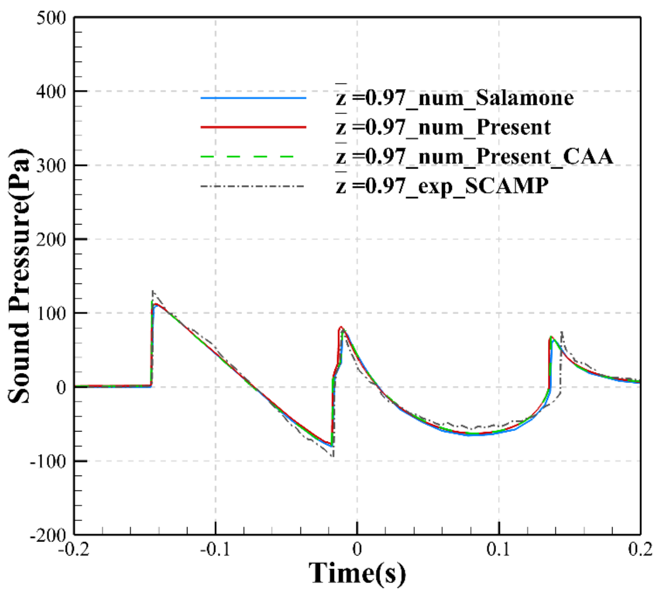

Figure 8 – Focus boom prediction at $\bar{z} = 0.97$

At $\bar{z} = 0.67$, the tail shock of the incoming wave and the head shock of the outgoing wave are combined, and the peak value of overpressure of the combined shock exceeds the incoming wave. Except that the duration of the U-shaped outgoing waveform is slightly shorter, the consistency of numerical prediction signal and the measured signal is good. The use of CAA techniques appears to have little effect on the prediction results.

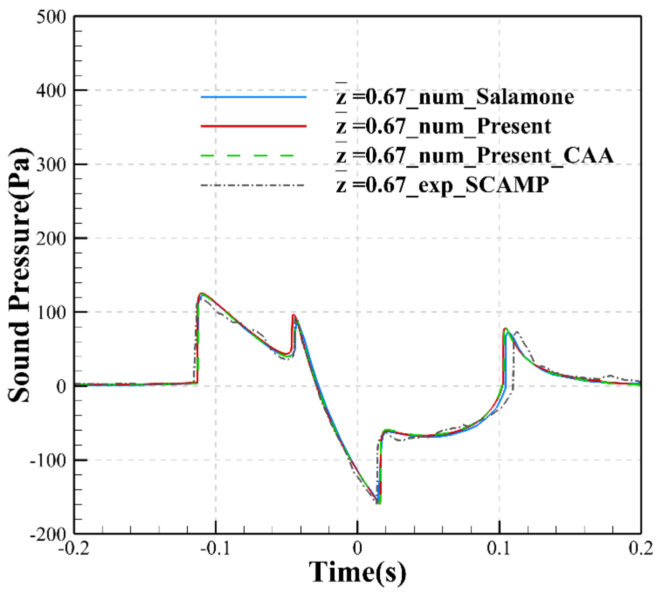

Figure 9 – Focus boom prediction at $\bar{z} = 0.67$

At $\bar{z} = 0.15$, the incoming wave and outgoing wave are completely merged. The maximum overpressure is 471.4Pa, so the amplification factor of the maximum overpressure of the focus boom is about 8.2. The overpressure of the numerical predicted head shock and tail shock are both overestimated, and the duration is also slightly smaller than the measured. The CAA result has better prediction on the amplitude of shock peak, but the duration is still smaller than the experimental result.

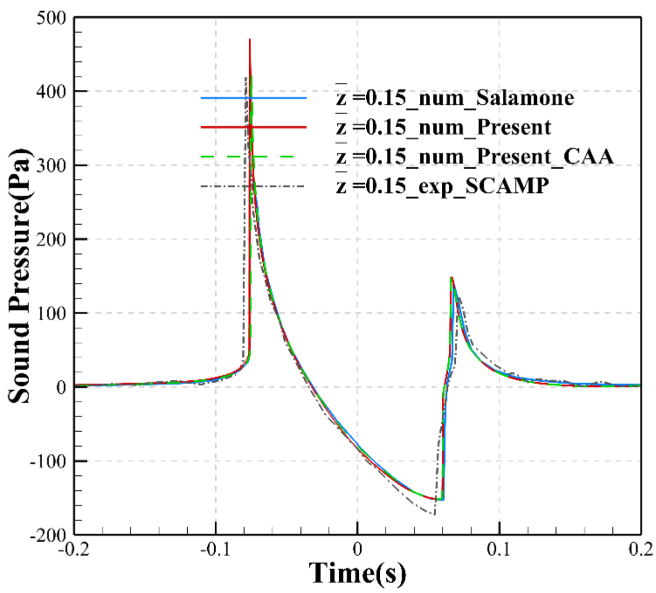

Figure 10 – Focus boom prediction at $\bar{z} = 0.15$

At $\bar{z} = -0.22$ shadow zone, the signal is smooth and there is no more shock wave. The peak value of the numerically predicted signal is smaller than the measured. The CAA result is slightly better for whole the waveform. In general, the numerical predicted results of the focus boom are basically consistent with the measured data of the SCAMP flight test, and CAA techniques can achieve better results than lower order scheme at some caustic normal locations.

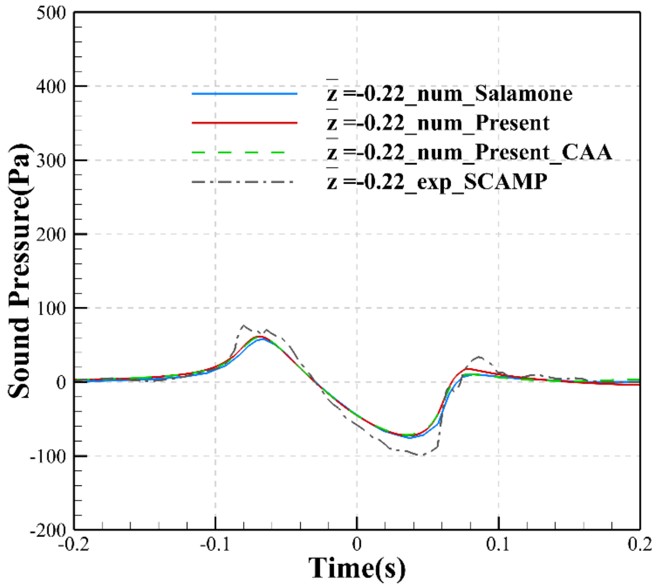

Figure 11 – Focus boom prediction at $\bar{z} = -0.22$

5. Discussion

5.1 Influence of Atmospheric Loss Mechanisms

Figure 12 demonstrates the effect of the atmospheric loss mechanism on the spectrum of the focus boom signal at $\bar{z} = 0.67$. In the low frequency range, due to the small atmospheric loss coefficient, the loss effect is weak. For the frequency exceeds 1000Hz, the spectrum amplitude considering the atmospheric loss mechanism is lower than that without the atmospheric loss mechanism, and this phenomenon is obvious in the frequency range from 3000Hz to 7000Hz. The Perceived Loudness (PLdB) of the focus boom signal considering the atmospheric loss mechanism is 111.3dB, and that without the atmospheric loss mechanism is 112.74dB. Because the human ear is more sensitive to medium and high frequency sounds, the effect of atmospheric loss is more significant in the middle and high frequencies. Therefore, although the most energy of the focus boom signal is in the low frequency range, the atmospheric loss mechanism reduces the PLdB by about 1.5dB, which reveals that the importance of atmospheric dissipation effect for the numerical prediction.

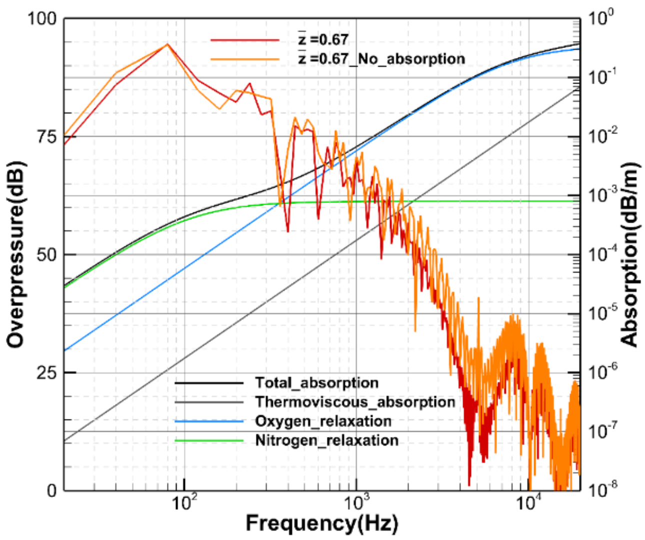

Figure 12 – Influence of atmospheric loss mechanism on focus boom spectrum

5.2 Influence of Caustics Normal Distance

Figure 13 shows the relation between maximum overpressure and PLdB with the normal distance to the caustic. In the focus zone, the maximum overpressure basically increases with the decrease of the normal distance to the caustic. The PLdB increases slowly, and increases rapidly near the peak. The maximum overpressure and PLdB both have two peaks, located at $\bar{z} = 0.15$ and $\bar{z} = 0.062$, respectively, corresponding to the head shock peak and tail shock peak of the merged U-shaped wave. In the shadow zone, the signals dissipate rapidly, the maximum overpressure and PLdB decrease rapidly. The maximum PLdB of the focus boom is located at $\bar{z} = 0.062$, which is nearly 20dB higher than that of the sonic boom produced by cruising flight. Supersonic maneuvering will greatly increase the sonic boom intensity in some spaces within the sonic boom footprint. Except near the two peaks, the PLdB of the focus boom is relatively low in the focus zone, which indicates that the region where the sonic boom intensity significantly increases due to the focus effect is small. By carefully designing appropriate flight trajectories, the high intensity area can be placed in an uninhabited area, so as to reduce the consideration of focus boom in the low-boom configuration design for supersonic civil aircraft.

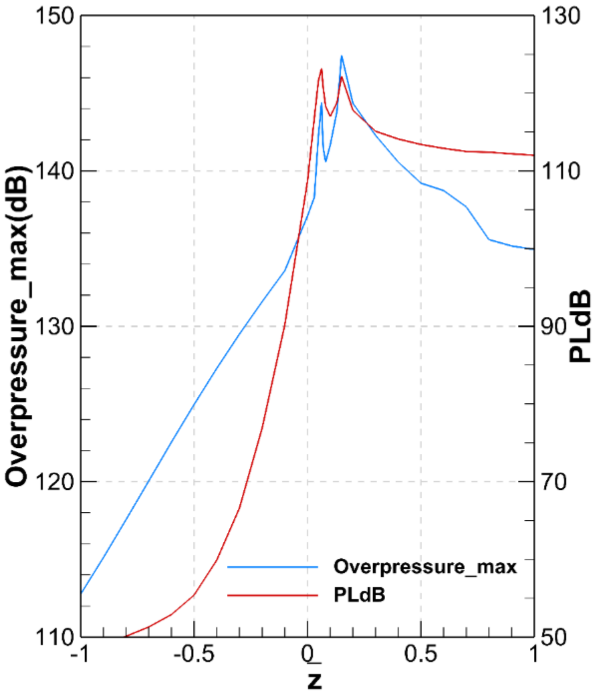

Figure 13 – Relation between PLdB and maximum overpressure to the normal distance

5.3 Influence of Flight Path Angle

The intensity of the focus boom is related to the aerodynamic shape, flight state and atmospheric profile. Since the focus boom produced by the accelerating process from subsonic to supersonic speed is unavoidable, it is particularly important to reduce the intensity of the focus boom in this condition. Changing the flight path angle (FPA) can change the spatial distribution of the sonic boom energy, thereby reducing its intensity. The effect of FPA on focus boom intensity was investigated using "Maneuver A", a level acceleration flight test in SCAMP [2]. The intensity of the focus boom in different FPA generated on the ground is calculated. Focus boom predictions for FPAs of $0, +1°, +3°$ were performed respectively. A positive angle is defined as climbing. The focus amplification factor is defined as the ratio of the maximum overpressure in the focus area to the maximum overpressure of the incoming wave, representing the intensity of the focus boom. Figure 14 shows the relationship between focus amplification factor and FPA. With the increase of FPA, the focus amplification factor gradually decreases, and the focus boom intensity weakens. A possible explanation is that in the climbing state, the sonic boom signal generated from the near field of the aircraft needs to propagate farther to reach the ground, and according to the geometric acoustics theory, the intensity of the sonic boom on the ground will be reduced. Therefore, climbing while accelerating might be a realistic method to reduce the impact of focus boom.

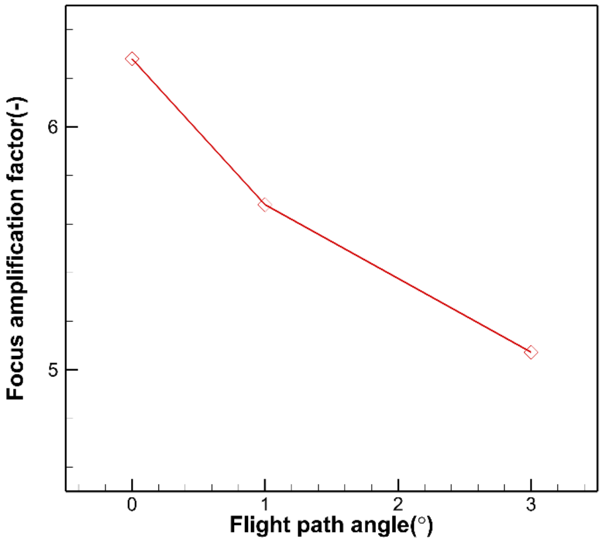

Figure 14 – The relationship between FPA and focus magnification factor

6. Conclusion

Numerical prediction of focus boom generated by maneuvers is studied. The numerical prediction method is studied and focus boom code CBoom_NLTE based on nonlinear Tricomi equation is developed. The code is verified by the flight data of SCAMP. The prediction results are in good agreement with the measured data. The atmospheric loss effects will dissipate the sonic boom energy in medium and high frequency. Since the human is more sensitive to the sound in this frequency band, the atmospheric loss effects need to be considered in the focus boom prediction. In the focus zone, the area where the perceived loudness increases significantly is very small. According to this feature, the focus boom issue might be solved through flight trajectory planning instead of aerodynamic design. Climbing while accelerating can reduce the intensity of focus boom, which might be a realistic method to reduce the impact of focus boom.

7. Contact Author Email Address

Shuo Han: hanshuo@cae.ac.cn

8. Copyright Statement

The authors confirm that they, and/or their company or organization, hold copyright on all of the original material included in this paper. The authors also confirm that they have obtained permission, from the copyright holder of any third party material included in this paper, to publish it as part of their paper. The authors confirm that they give permission, or have obtained permission from the copyright holder of this paper, for the publication and distribution of this paper as part of the ICAS proceedings or as individual off-prints from the proceedings.

References

[1] Stevens S S. Perceived level of noise by Mark VII and decibels(E). *Journal of the Acoustical Society of America*, Vol. 51, No. 2B, pp 575-601, 1972.

[2] Page J. Superboom Caustic analysis and measurement program (SCAMP) Final Report. *NASA/CR-2015–218871*, California, 2015.

[3] Brekhovskikh L M. *Waves in layered media*. 2nd edition, Academic Press, 1980.

[4] Berry M V. Waves and thom's theorem. *Advances in Physics*, 1976, Vol 25, No. 1, pp 1-26, 1976.

[5] Guiraud J P. Acoustique géométrique, bruit balis-tique des avions supersoniques et focalization. *Journal de Mécanique*, Vol 4, No 2, pp 215-267, 1965.

[6] Plotkin K J and Cantril J M. Prediction of sonic boom at a focus. *AIAA 14th Aerospace Sciences Meeting*, Washington D. C, Vol. 76, 2, pp 1-15, 1976.

[7] Auger T and Coulouvrat F. Numerical simulation of sonic boom focusing. *AIAA Journal*, Vol. 40, N0. 9, pp 1726-1734, 2002.

[8] Marchiano R, Coulouvrat F and Crenon R. Numerical simulation of shock wave focusing at fold caustics, with application to sonic boom. *Journal of the Acoustical Society of America*, Vol. 114, No. 4, pp 1758-1771, 2003.

[9] Hayes W D, Haefeli R C and Kulsrud H E. Sonic boom propagation in a stratified atmosphere with computer program. *NASA CR-1299*, Washington D. C, 1969.

[10] Sescu A and Afjeh A A. On the Discontinuous Ga-lerkin computation of N-waves focusing. *International Journal for Numerical Methods in Fluids*, Vol. 67, No. 11, pp 1758-1768, 2011.

[11] Salamone III J A, Sparrow V W and Plotkin K J. Solution of the lossy nonlinear Tricomi equation applied to sonic boom focusing. *AIAA journal*, Vol. 51, No. 7, pp 1745-1754, 2013.

[12] McDonald B E and Ambrosiano J. High-order upwind flux methods for scalar hyperbolic conservation laws. *Journal of Computational Physics*, Vol. 56, No. 3, pp 448-460, 1984.

[13] Salamone III J A. Solution of the lossy nonlinear Tricomi equation with application to sonic boom focus-ing. State College: The Pennsylvania State University, 2013.

[14] Tam C K W and Webb J C. Dispersion-Relation-Preserving Finite Difference Schemes for Computational Acoustics. *Journal of Computational Physics*, Vol. 107, No. 2, pp 262-281, 1993.

[15] Stanescu D and Habashi W G. 2N-Storage Low Dissipation and Dispersion Runge-Kutta Schemes for Computational Acoustics. *Journal of Computational Physics*, Vol. 143, No. 2, pp 674-681, 1998.